European Journal of Nuclear Medicine and Molecular Imaging (2019) 46:2581–2589
https://doi.org/10.1007/s00259-019-04477-3

ORIGINAL ARTICLE

Non-invasive prediction of *IDH*-wildtype genotype in gliomas using dynamic ^{18}F-FET PET

Franziska Vettermann[1,2] · Bogdana Suchorska[2,3] · Marcus Unterrainer[1,2] · Debie Nelwan[1] · Robert Forbrig[4] · Viktoria Ruf[5] · Vera Wenter[1] · Friedrich-Wilhelm Kreth[2,3] · Jochen Herms[5] · Peter Bartenstein[1,2] · Jörg-Christian Tonn[2,3] · Nathalie L. Albert[1,2]

Received: 12 April 2019 / Accepted: 2 August 2019 / Published online: 13 August 2019

Abstract

Purpose According to the updated WHO classification of gliomas with its emphasis on molecular parameters, tumours with an *IDH*-wildtype status have a dismal prognosis. To ensure timely adjustment of treatment, demand for non-invasive prediction methods is high. ^{18}F-FET PET has been shown to be an important diagnostic tool for glioma management. The aim of this study was to assess the value of dynamic ^{18}F-FET PET for the non-invasive prediction of the *IDH*-mutation status.

Methods Newly diagnosed WHO grade II–IV glioma patients with MRI and dynamic ^{18}F-FET PET were included. The ^{18}F-FET PET parameters mean and maximal tumour-to-background ratio (TBR_{mean}, TBR_{max}) and minimal time-to-peak (TTP_{min}) were evaluated. The diagnostic power for the prediction of the *IDH* genotype (positive/negative predictive value) was tested in the overall study group and in the subgroup of non-contrast enhancing gliomas.

Results Three hundred forty-one patients were evaluated. Molecular analyses revealed 178 *IDH*-mutant and 163 *IDH*-wildtype tumours. Overall, 270/341 gliomas were classified as ^{18}F-FET-positive ($TBR_{max} > 1.6$), 90.2% of the *IDH*-wildtype and 69.1% of *IDH*-mutant gliomas. Median TBR_{max} was significantly higher in *IDH*-wildtype compared with *IDH*-mutant gliomas (2.9 vs. 2.3, $p < 0.001$); however, ROC-analyses revealed no reliable cutoff due to a high overlap (range 1.0–7.1 vs. 1.1–7.9). Dynamic analysis revealed a significantly shorter TTP_{min} in *IDH*-wildtype gliomas; using $TTP_{min} \leq 12.5$ min as indicator for *IDH*-wildtype gliomas, a positive predictive value of 87% was reached (negative predictive value 72%, AUC = 0.796, $p \leq 0.001$). A total of 161/341 gliomas did not show contrast enhancement on MRI; even within this subgroup, $TTP_{min} \leq 12.5$ min remained a good predictor of *IDH*-wildtype glioma (positive predictive value 83%, negative predictive value 90%; AUC = 0.868, $p < 0.001$).

Conclusion A short TTP_{min} in dynamic ^{18}F-FET PET serves as good predictor of highly aggressive *IDH*-wildtype status in gliomas. In particular, a high diagnostic power was observed in the subgroup of non-contrast enhancing gliomas, which helps to identify patients with worse prognosis.

Keywords Glioma · ^{18}F-FET PET · Non-invasive grading · *IDH* mutation status

Franziska Vettermann and Bogdana Suchorska contributed equally to this work.

This article is part of the Topical Collection on Oncology – Brain

Electronic supplementary material The online version of this article (https://doi.org/10.1007/s00259-019-04477-3) contains supplementary material, which is available to authorized users.

✉ Nathalie L. Albert
Nathalie.albert@med.uni-muenchen.de

[1] Department of Nuclear Medicine, University Hospital, Ludwig Maximilians-University Munich, Munich, Germany

[2] German Cancer Consortium (DKTK), partner site Munich, German Cancer Research Center (DKFZ), Heidelberg, Germany

[3] Department of Neurosurgery, University Hospital, Ludwig Maximilians-University Munich, Munich, Germany

[4] Department of Neuroradiology, University Hospital, Ludwig Maximilians-University Munich, Munich, Germany

[5] Center for Neuropathology and Prion Research, Ludwig-Maximilians-University Munich, Munich, Germany

Introduction

Gliomas show a large histopathological and genetic heterogeneity, which is a critical aspect in their classification or when estimating the aggressiveness of the lesion and determining the patients' clinical management [1, 2]. In the past, glioma classification was largely based on their phenotype, resulting from microscopically derived features such as cell proliferation, mitosis, necrosis or their similarities with different cells of origin and their differentiation [3]. With its emphasis on molecular parameters such as *IDH*-mutation and co-deletion on chromosomes 1p and 19q, the 2016 revision of the World Health Organization (WHO) has led to a paradigm shift in glioma classification [4]. Basically, this shift resulted in the establishment of two heterogeneous groups: *IDH*-mutant tumours, which can be subdivided into astrocytic (without 1p/19q co-deletion) or oligodendroglial (harbouring 1p/19q co-deletion) tumours, and *IDH*-wildtype gliomas (glioblastoma or glioblastoma-like lesions). The prognosis of patients with newly diagnosed glioma now strongly depends on this molecular classification and will result in increasingly individualised treatment concepts [5]. Besides structural magnetic resonance imaging, molecular imaging using ^{18}F-FET PET has proven helpful in characterisation of glial lesions, not only in terms of surgical procedure or radiation therapy planning but also providing important imaging biomarkers, which help with non-invasive glioma grading and prediction of prognosis [6–9]. So far, only few studies have focussed on non-invasive glioma "grading" according to the new WHO 2016 classification [10, 11]. Our group has previously shown dynamic ^{18}F-FET PET analysis using time-to-peak (TTP), which depicts the time of the maximum influx of the tracer into the tumour cells, to be correlated with both conventional gradings as well as prognosis. Thus, for the present study, we aimed at evaluating the predictive value of static and dynamic ^{18}F-FET PET parameters for the prediction of an *IDH*-wildtype status in WHO grade II-IV glioma.

Material and methods

Patients

Patients with newly diagnosed, histopathologically confirmed glioma with a concurrent MRI and dynamic ^{18}F-FET PET scan prior to further therapy were included retrospectively. Written consent was obtained from all patients; the study was approved by the local ethics committee (approval number 604-16).

PET acquisition and mode of evaluation

On average, 180 MBq ^{18}F-FET were injected as an intravenous bolus. Forty-minute dynamic ^{18}F-FET PET scans (16 frames) were acquired with an ECAT Exact HR+ scanner (Siemens, Erlangen, Germany) according to standard protocols and evaluated on a Hermes workstation (Hermes Medical Solutions, Stockholm, Sweden) as described previously [12]. For the assessment of the maximal and mean tumour to background ratio (TBR_{max}, TBR_{mean}), the maximal and mean standardized uptake value (SUV) of the tumour was corrected for the mean background activity in the healthy, contralateral hemisphere [13]. Tumours were termed ^{18}F-FET-positive, when TBR_{max} was above 1.6 and ^{18}F-FET-negative when TBR_{max} was below 1.6 [14, 15].

Biologic tumour volume (BTV) was evaluated by semiautomatic threshold-based delineation of a volume of interest using the published threshold $SUV_{BG} \times 1.6$ [7].

Within the 40-min dynamic scan, time-to-peak (TTP) was assessed in each slice within the tumour and consequently the shortest TTP in at least two consecutive slices was defined as minimal TTP (TTP_{min}) [9]. Regarding the exclusion of noise artefacts in the beginning of the PET acquisition due to low counting rates, only slices 11–16 (3–40-min p.i.) were analysed in the dynamic evaluation. According to the length of our frames, TTP_{min} is appointed for 4, 7.5, 12.5, 17.5, 25, and 35 min in frame 11–16, respectively.

Magnetic resonance imaging

Patients underwent routine MR imaging scans with either a 1.5-T (Magnetom Symphony; Siemens, Erlangen, Germany) or a 3.0-T (Signa HDx, 3 T; GE Healthcare, Milwaukee, WI) scanner. Axial T2-weighted sequences as well as T1-weighted sequences before and after intravenous administration of 0.1-mmol/kg gadobenatedimeglumine contrast agent (Gd-BOPTA, MultiHance; BraccoImaging, Milan, Italy) were acquired. Images were read and interpreted by an experienced radiologist (R.F.) using a PACS workstation (Sienet Magic View 1000; Siemens). Tumours were classified as contrast-enhancing (CE), whenever contrast medium was detectable within the tumour and not related to vascular structures, independent of its size.

Histopathological evaluation and immunohistochemistry

PET-guided stereotactic biopsy procedures or neuronavigated microsurgery with MR imaging and PET image fusion (Brainlab, Heimstetten, Germany) were used to ensure a spatially precise tissue-sampling procedure throughout the tumour. Histologic classification, immunochemistry and tumour grading were performed according

to the current WHO guidelines by an experienced neuropathologist, as previously described [16] [4]. For immunohistochemical staining, 5-μm tissue sections of formalin-fixed paraffin-embedded tumour samples were pretreated with CC2 for 60 min followed by incubation with anti-*IDH1* (R132H) mouse monoclonal antibody (IHC 132, GenomeMe, Richmond, BC, Canada, dilution 1:100 (antibody diluent from DCS, Hamburg, Germany)) for 32 min. Staining was performed on a Ventana Benchmark Ultra autostainer with the iView DAB Kit (Ventana Medical Systems). Slides were counterstained with haematoxylin. *IDH*-status from the immuno-histochemical staining was confirmed by sequencing.

Statistical analysis

Statistical analysis was performed with IBM® SPSS® Statistics, Version 25. Descriptive statistics were used for patients' characteristics and ^{18}F-FET PET data (TTP_{min} and TBR_{max}).

Diagnostic power was evaluated by receiver operating characteristic (ROC) analysis including areas under the curve (AUC). The positive predictive value (PPV), negative predictive value (NPV) and accuracy (ACC) as well as the sensitivity (sens) and specificity (spec) were calculated in the overall group as well as in different subgroups (e.g., ^{18}F-FET-positive gliomas only; non-contrast enhancing gliomas). For the evaluation of different TTP_{min} thresholds, which can be assessed in ^{18}F-FET-positive gliomas only, as indicator for an *IDH*-wildtype status, the ^{18}F-FET-negative cases were added to the $TTP_{min} > 35$-min subgroup. Statistical significance was defined as a two-tailed p value of < 0.05.

Results

Patients characteristics

Three hundred forty-one adult patients (196 men, 145 women; mean age 48.8 ± 15.2 years) with a primary diagnosis of WHO grade II, III and IV glioma were included in the study. Histopathological analyses revealed 163 *IDH*-wildtype and 178 *IDH*-mutant gliomas (97/178 *IDH*-mutant without 1p/19q-codeletion, 81/178 *IDH*-mutant with 1p/19q-codeletion gliomas). Two hundred eighty-six patients underwent stereotactic biopsy and 55 patients microsurgical resection after undergoing ^{18}F-FET-PET. Overall, 52.8% (180/371) of patients presented with a contrast enhancement (CE) on MRI, 74.2% (121/163) of the *IDH*-wildtype and 33.1% (59/178) of the *IDH*-mutant gliomas.

Static ^{18}F-FET PET parameters

Overall, 79% (270/341) gliomas showed ^{18}F-FET-uptake with a $TBR_{max} > 1.6$, referred to as ^{18}F-FET-positive, and 21% (71/341) gliomas were ^{18}F-FET-negative. In the molecular genetic subgroup of *IDH*-wildtype gliomas, 90.2% (147/163) showed an ^{18}F-FET-uptake. Of the *IDH*-mutant gliomas, only 69.1% (123/178) were ^{18}F-FET-positive (47.4% (46/97) of the *IDH*-mutant gliomas without 1p/19q-codeletion, 95.1% (77/81) of the *IDH*-mutant gliomas with 1p/19q).

Among the ^{18}F-FET-positive gliomas, median TBR_{max} was 3.0 (range 1.6–7.9), median TBR_{mean} was 2.0 (range 0.3–20.1) and median BTV was 16.4 ml (range 0.1–133.3). *IDH*-wildtype gliomas presented with a high median TBR_{max} of 3.1 (range 1.7–7.1), median TBR_{mean} of 2.1 (range 1.1–20.1) and a median BTV of 17.4 ml (range 0.2–133.3). In contrast, *IDH*-mutant gliomas showed a significantly lower median TBR_{max} of 2.7 (range 1.6–7.9; $p = 0.009$) and a significantly lower median TBR_{mean} of 1.9 (range 0.3–4.1; $p = 0.039$). The median BTV of 15.6 ml (range 0.1–115.2) did not significantly differ from *IDH*-wildtype gliomas ($p = 0.295$).

For detailed information of the subgroups, please refer to Table 1.

ROC-analyses using TBR_{max} (AUC 0.593, $p = 0.009$), TBR_{mean} (AUC 0.560, $p = 0.093$) and BTV (AUC 0.540, $p = 0.262$) among ^{18}F-FET-positive cases revealed no reliable cutoff value for the differentiation between *IDH*-wildtype and *IDH*-mutant gliomas (Fig. 1). Significant AUC was seen using TBR_{max}, resulting in the best cutoff at TBR_{max} 2.6, which, however, led to a low accuracy due to a high overlap of TBR_{max} values between the groups (Joudens-J 0.3, PPV 44%, NPV 39%, ACC 41%, sens 31%, spec 54%).

^{18}F-FET-negative gliomas were in 77.5% (55/71) of cases *IDH*-mutant and in only 22.5% (16/71) of cases *IDH*-wildtype. ^{18}F-FET-negativity predicted an *IDH*-mutation with a NPV of 77%. ROC-analysis for TBR_{max} including ^{18}F-FET-negative cases revealed no significant cutoff value (AUC = 0.625, $p = 0.131$). TBR_{mean} and BTV as well as TTP_{min} could not be assessed due to missing ^{18}F-FET-uptake.

Table 1 Static PET-parameters in *IDH*-wildtype and *IDH*-mutant, ^{18}F-FET-positive gliomas; median TBR_{max} (range), median TBR_{mean} (range), median BTV (range)

	TBR_{max}	TBR_{mean}	BTV [ml]
IDH-wildtype	3.1 (1.7–7.1)	2.1 (1.1–20.1)	17.4 (0.2–133.3)
IDH-mutant	2.7 (1.6–7.9)	1.9 (0.3–4.1)	15.6 (0.1–125.3)
Group comparison (p value)	0.009	0.039	0.295

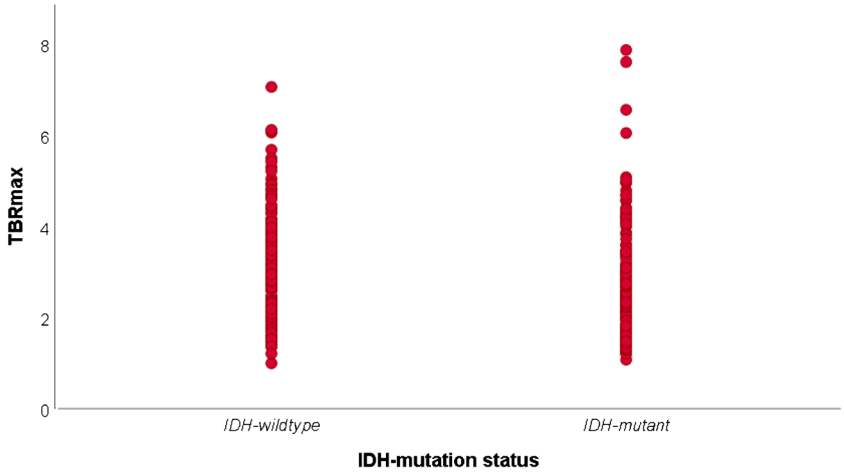

Fig. 1 Scatter chart of TBR_{max} distribution in *IDH*-wildtype versus *IDH*-mutant gliomas showing the high overlap between both groups

Dynamic ^{18}F-FET PET parameters

^{18}F-FET uptake dynamics were evaluated in ^{18}F-FET-positive cases only ($n = 270$). *IDH*-wildtype gliomas had a significantly shorter median TTP_{min} of 12.5 min (range 7.5–35 min) compared with TTP_{min} of 25 min (range 7.5–35 min) in *IDH*-mutant gliomas ($p < 0.001$) (Table 2).

Using the different time points in dynamic PET, the best differentiation between *IDH*-wildtype and *IDH*-mutant gliomas was achieved using $TTP_{min} \leq 12.5$ min as indicator for an *IDH*-wildtype with particularly high positive predictive value and specificity (PPV 87%, NPV 72%, ACC 79%, sens: 72%, spec 87%). The highest specificity was found at the cutoff $TTP_{min} \leq 7.5$ min, but with a very low sensitivity (PPV 90%, NPV 52%, ACC 58%, sens 25%, spec 97%). Reversely, the highest sensitivity was found at a cutoff $TTP_{min} \leq 25$ min (PPV 62%, NPV 80%, ACC 66%, sens 93%, spec 33%). For further specification, see Table 3.

Considering a long TTP_{min} or ^{18}F-FET-negativity as an indicator for *IDH*-mutation and a short TTP_{min} as indicator for an *IDH*-wildtype, in the entire group of patients including the ^{18}F-FET-negative cases, the highest ACC was detected using $TTP_{min} \leq 12.5$ min with 79% (PPV 87%, NPV 74%, sens 65%, spec 91%).

Diagnostic power in non-contrast enhancing gliomas

In 40% (65/161) of cases, non-CE gliomas were ^{18}F-FET-negative. The calculation of all values (PPV/NPV/ACC/sens/spec) in the group of ^{18}F-FET-positive glioma yielded comparable results as those in the overall group (Supplement Tables 1 and 2).

Using the different time points in dynamic PET in the entire group including ^{18}F-FET-negative cases, the highest ACC for the differentiation of *IDH*-mutational status was again detected using $TTP_{min} \leq 12.5$ min with 84% (PPV 83%, NPV 84%, sens 48%, spec 97%) (see Figs. 2 and 3).

Diagnostic power in WHO grade II and III gliomas

To take into account the inter-correlation of grading and molecular features, we aimed at detecting the *IDH*-wildtype status in the subgroup of WHO grade II/III glioma only.

Table 2 Number of *IDH*-wildtype and *IDH*-mutant gliomas in each subgroup divided by TTP_{min}, in the overall group and in the non-contrast-enhancing group only

Overall group					
All (CE and non-CE gliomas)			Non-CE gliomas only		
TTP_{min} [minutes]	*IDH*-wildtype	*IDH*-mutant	TTP_{min} [minutes]	*IDH*-wildtype	*IDH*-mutant
≤7.5	37	4	≤7.5	4	0
12.5	69	12	12.5	16	4
17.5	22	36	17.5	2	19
25	9	31	25	2	16
35	10	40	35	3	30
^{18}F-FET-negative	16	55	^{18}F-FET-negative	15	50

CE contrast enhancement

Table 3 Dynamic evaluation in the overall study group with and without contrast enhancing (CE) gliomas and in the subgroup of non-contrast enhancing (non-CE) gliomas only

Overall group									
All (CE and non-CE gliomas)					Non-CE gliomas only				
TTP_{min} [minutes]	≤ 7.5	≤ 12.5	≤ 17.5	≤ 25	TTP_{min} [minutes]	≤ 7.5	≤ 12.5	≤ 17.5	≤ 25
PPV %	90	87	71	62	PPV %	100	83	49	38
NPV %	58	74	78	78	NPV %	76	84	83	81
Accuracy	62	79	74	68	Accuracy	76	84	73	64
Sensitivity %	23	65	79	84	Sensitivity %	10	48	52	57
Specificity %	98	91	71	53	Specificity %	100	97	81	67

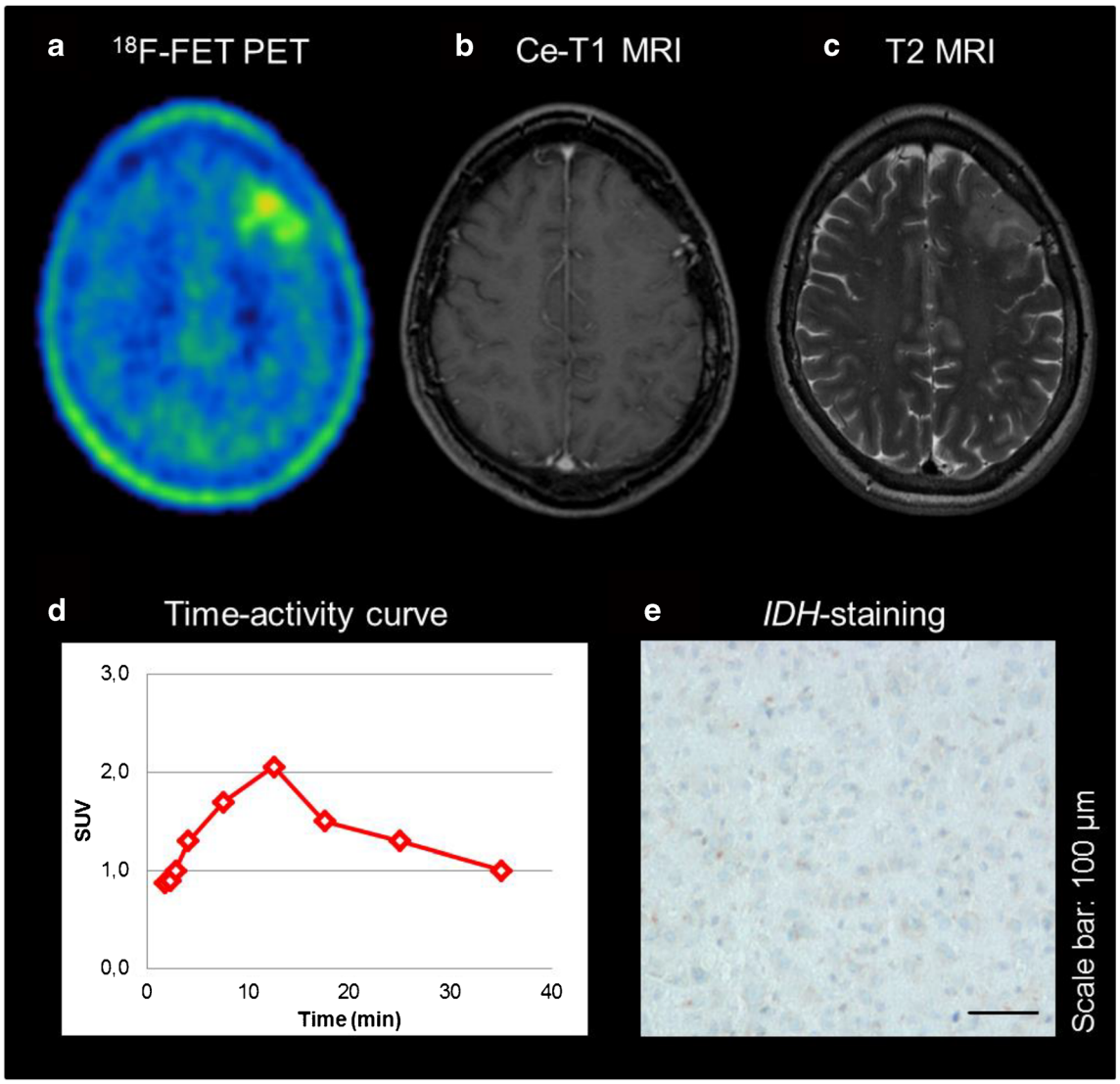

Fig. 2 Example of a patient with a ^{18}F-FET-positive lesion in the left frontal lobe, moderate TBR_{max} 2.1 and rather small BTV of 6.5 ml (A) without contrast-enhancement in CE-T1 MRI (B) and a T2 alteration in T2 MRI (C) but with a short TTP_{min} of 12.5 min; histopathological analysis revealed an *IDH*-wildtype, anaplastic astrocytoma (WHO grade III)

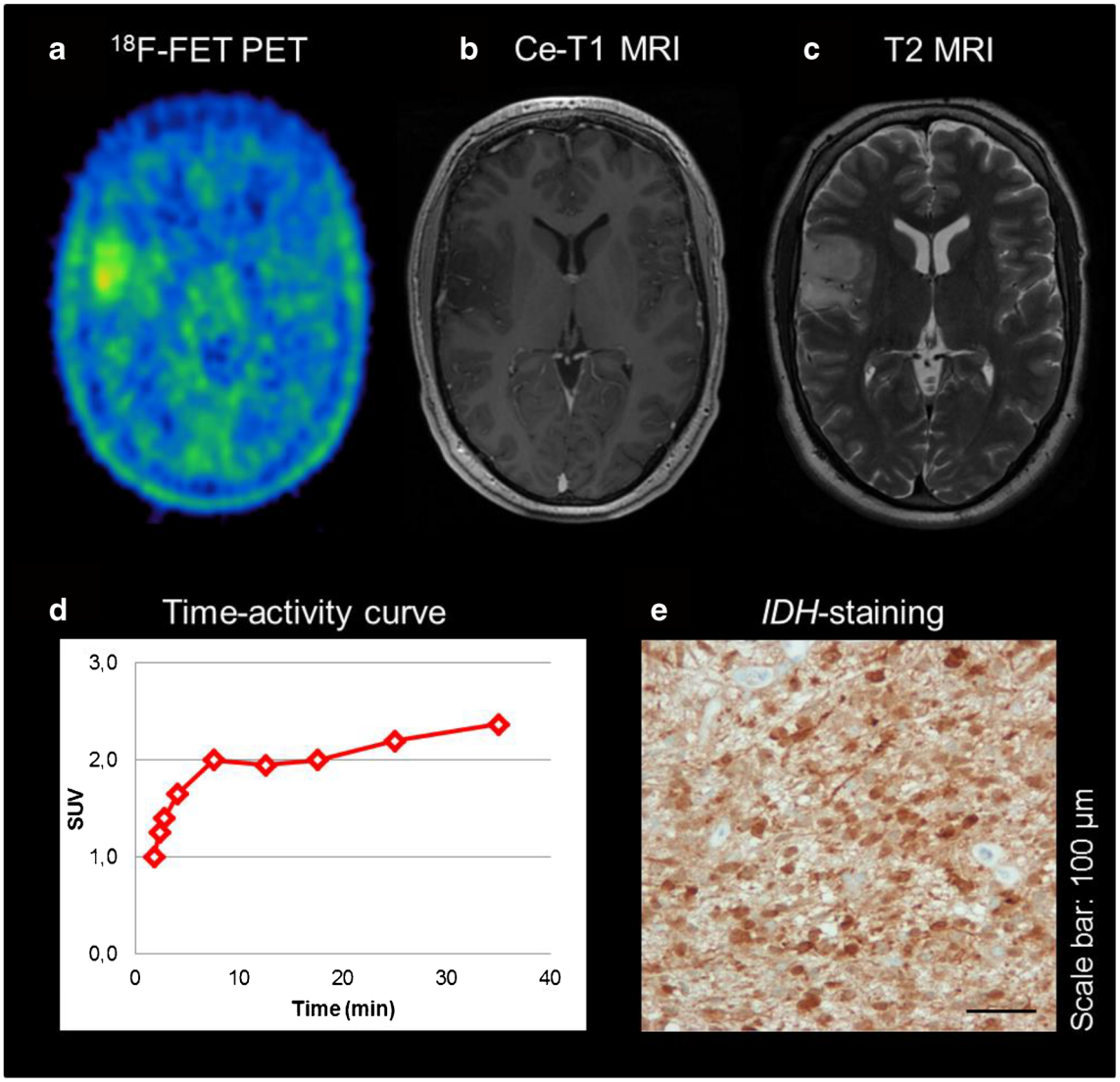

Fig. 3 Example of a patient with a ^{18}F-FET-positive lesion in the right temporoparietal lobe, moderate TBR_{max} 2.2 and rather small BTV of 6.8 ml **a** without contrast-enhancement in CE-T1 MRI **b** and a small T2 alteration in T2 MRI **c** and with a long TTP_{min} (35 min) and an increasing time-activity curve; histopathological analysis revealed an *IDH*-mutant, diffuse astrocytoma (WHO grade II)

In the ^{18}F-FET-positive group only, using the different time points in dynamic PET, the highest ACC was detected using $TTP_{min} \leq 12.5$ min with 83% (sens 72%, spec 89%, PPV 77%, NPV 86%).

Using the different time points in dynamic PET including ^{18}F-FET-negative cases, the best results were detected using $TTP_{min} \leq 12.5$ min as indicator for an *IDH*-wildtype with an ACC of 81% (PPV 77%, NPV 83%, sens 57%, spec 92%; Table 4).

Diagnostic power in gliomas with lower ^{18}F-FET-uptake ($TBR_{max} < 2.6$)

Dividing the group using the median split of TBR_{max} we were able to only look at ^{18}F-FET-positive gliomas with lower FET-uptake ($TBR_{max} < 2.6$; $n = 171$). In this subgroup, the time point of $TTP_{min} \leq 12.5$ min could differentiate between *IDH*-wildtype and *IDH*-mutant gliomas with an even higher ACC of 81% (PPV 91%, NPV 77%, sens 64%, spec 95%).

Discussion

Non-invasive tumour grading is gaining further importance for the detection and characterization of multiple neoplastic lesions. The advent of numerous new molecular markers, such as genetic alterations or changes in protein structure or functions, demands fast translation of the knowledge in the underlying molecular biology into clinical practice, as these alterations might affect the disease course. Furthermore, different molecular pathways often result in a modified metabolism,

Table 4 Dynamic evaluation in the subgroup of only WHO grade II and III gliomas with and without CE and in the subgroup of only non-contrast enhancing glioma

WHO grade II / III									
All (CE and non-CE gliomas)					Non-CE gliomas only				
TTP_{min} [minutes]	≤ 7.5	≤ 12.5	≤ 17.5	≤ 25	TTP_{min} [minutes]	≤ 7.5	≤ 12.5	≤ 17.5	≤ 25
PPV %	80	77	53	42	PPV %	100	83	48	37
NPV %	73	83	83	81	NPV %	76	84	83	81
Accuracy	74	81	71	60	Accuracy	77	84	73	64
Sensitivity %	21	57	68	71	Sensitivity %	10	46	51	56
Specificity %	98	92	73	55	Specificity %	100	97	81	67

which can be used for non-invasive visualization using metabolic imaging techniques such as positron emission tomography. In the field of primary brain tumours, especially glioma, current research focusses on molecular alterations such as *IDH*-mutation and co-deletion on chromosomes 1p/19q, which might pinpoint to distinct origins of these tumours [17–20]. Particularly interesting for the management and prognosis is the mutation in the *IDH*-gene, which can stratify glial tumours into two groups: those with a more favourable outcome harbouring an *IDH*-mutation and the other group with a dismal disease course lacking a mutation in this particular gene [17]. *IDH*-wildtype glioma, independent of their actual grading, seem to exhibit a clinical course which is comparable to primary glioblastoma, and thus have been also termed "glioblastoma-like-lesions" [18]. While primary glioblastoma mostly show a characteristic appearance on conventional MR imaging with the intense, contrast-enhancing, ring-like outer rim and a necrotic central zone, *IDH*-wildtype glioblastoma-like-lesions, especially in case of a lack of contrast enhancement, might mimic rather benign lower-grade glioma. A fast and non-invasive diagnostic method identifying these tumours with a high accuracy is needed in order to prevent delayed treatment. The present study has utilized time-to-peak-analysis obtained from dynamic ^{18}F-FET PET in order to identify these *IDH*-wildtype lesions within a large cohort of newly diagnosed glioma patients.

Using TTP_{min} analysis with a cutoff value of ≤ 12.5 min, we were able to identify *IDH*-wildtype tumours with a positive predictive value of 87% and an overall accuracy of 79% in the entire patient collective. As most WHO grade IV tumours are likely to be primary glioblastoma without a concurrent *IDH*-mutation, we have performed a separate analysis within the WHO grade II and III group only. In this subgroup, the accuracy of dynamic ^{18}F-FET PET remained sensibly high with 81%. Furthermore, we have analysed contrast-enhancing and non-enhancing gliomas separately; importantly, the prediction of the *IDH*-wildtype status was even possible with a high accuracy (84%) in the non-CE group, which represents a challenging and clinically interesting group, as the lack of CE on MRI would generally suggest a less aggressive glioma.

In order to increase the predictive value of dynamic FET-PET by combining TBR_{max} and TTP_{min}, we divided the overall group into gliomas with low versus high TBR_{max} and separately analysed the predictive value of TTP_{min} in both groups. Interestingly, in the subgroup of gliomas with low TBR_{max} (< 2.6), TTP_{min} was able to predict an *IDH*-wildtype status with a very high probability of 91%.

In general, the probability of an *IDH*-wildtype status was inversely correlated with the TTP_{min}, i.e. the shorter the TTP_{min}, the higher is the risk of an *IDH*-wildtype status. For example, a glioma with a TTP_{min} of 7.5 min has a 90% probability of an *IDH*-wildtype status and at a TTP_{min} of 12.5 min an 87% probability. This is due to the fact that *IDH*-mutant gliomas barely show a short TTP_{min}. Conversely, particularly in the group including CE gliomas, a certain number of *IDH*-wildtype gliomas (WHO grade II-IV) also present with a later TTP_{min}, resulting in a limited overall sensitivity for the detection of *IDH*-wildtype gliomas. However, for the interpretation of PET data in the clinical routine, the positive and negative predictive values are important factors determining the further clinical management of an individual patient. Therefore, in case of a short TTP_{min}, a highly aggressive *IDH*-wildtype glioma can be presumed with high certainty and urgent therapy planning in clinical routine needs to follow, even if a patient presents without contrast enhancement on MRI and might otherwise classify for a watch-and-wait strategy.

The non-invasive prediction of an *IDH*-wildtype status in suspected low-grade glioma is of utmost clinical importance, as many of these tumours do not enhance on initial MRI and are often considered "benign lesions" leading to a watch-and-wait strategy. Thus, dynamic PET might provide a risk assessment for a probability of an *IDH*-wildtype tumour and lead to a faster therapy initiation in these patients. In contrast to the dynamic evaluation, evaluation of static parameters such as TBR_{max}, TBR_{mean} or BTV did not provide comparable results for differentiation between *IDH*-mutant and *IDH*-wildtype tumours in our study. The biological background as of why *IDH*-wildtype

tumours tend to present with very short TTP_{min} times has yet to be elucidated. A possible explanation might be either a higher expression of the large amino acid transporter 1 (LAT1) which is responsible for intracellular uptake of ^{18}F-FET but has not been correlated with the molecular signature of gliomas so far, or an elevated perfusion (or possibly a combination of both aspects) in *IDH*-wildtype glioma compared with *IDH*-mutant ones [16].

So far, only a small number of studies exist examining the value of static and dynamic ^{18}F-FET PET for non-invasive characterization of *IDH*-mutation status in newly diagnosed glioma [11, 21]. Verger et al. have shown in a cohort of 90 patients that a combination of static and dynamic PET parameters provides a tool to predict the *IDH*-mutation status. The accuracy of dynamic ^{18}F-FET PET using TTP to predict *IDH*-mutation was 72%. A recent study by Lohmann et al. has evaluated a radiomics approach to ^{18}F-FET PET data and has found that a combination of a dynamic parameter (slope) with textural analysis has provided the highest accuracy (81%) for prediction of an *IDH*-mutation. These findings are in line with the results of our study, which comprises a higher number of included patients. In contrast to these two studies, we focused on the prediction of the *IDH*-wildtype status and not on the *IDH*-mutation, as the *IDH*-wildtype constitutes the group at risk. Furthermore, our cohort comprised a well-balanced number of both *IDH*-mutant ($n = 178$) and *IDH*-wildtype ($n = 163$) status tumours.

Comparing our results to MR spectroscopy identifying 2-hydroxyglutarate (2-HG), a metabolite which accumulates in case of a deficient *IDH*-enzyme, we have to point out that MRI spectroscopy provides very divergent results concerning sensitivity for prediction of *IDH*-mutation status, as the method is tumour volume dependent [19, 20]. In small tumours (< 8 ml) the sensitivity has been reported to be as low as 1%. Another study on an MRI-based method employing 7-Tesla-based relaxation-compensated multipool chemical exchange saturation transfer (CEST) MRI provided high specificity and sensitivity values for the prediction of the *IDH*-mutation status in 31 glioma patients [22]. However, 74% of the patients examined in that study were *IDH*-wildtype glioblastoma. Furthermore, use of 7-Tesla MRI scanners is rarely available for clinical routine. An interesting option for future studies would be to combine MRI and PET assessment, e.g. using a combined PET/MRI scanner.

Limitations of the study arise from the retrospective, single-centre study design; hence, the value of a TTP_{min}-based cutoff analysis for prediction of the *IDH* mutation status needs to be confirmed in larger, preferably multicentre, prospective studies**.** Furthermore, a technical limitation has to be mentioned: as dynamic FET-PET was not acquired in list mode but in previously fixed frames, TTP_{min} could only be evaluated in groups (7.5, 12.5, 17.5, 25, and 35 min).

Conclusion

A short TTP_{min} in dynamic ^{18}F-FET PET predicts an *IDH*-wildtype status with high probability even in non-contrast enhancing gliomas. Conventional static evaluation does not yield comparably good differentiation results. Dynamic ^{18}F-FET PET therefore provides an accurate and non-invasive tool for the identification of high-risk glioma harbouring an *IDH*-wildtype status and might lead to a faster therapy initiation in these tumours.

Funding information This work was supported by the Collaborative Research Centre SFB-824 of the Deutsche Forschungsgemeinschaft (DFG) and by the Else Kröner-Fresenius-Stiftung.

Compliance with ethical standards

Conflict of interest The authors declare that they have no conflict of interest.

Research involving human participants All procedures performed in studies involving human participants were in accordance with the ethical standards of the institutional and/or national research committee (local ethic committee - approval number 604-16) and with the 1964 Helsinki declaration and its later amendments or comparable ethical standards.

Informed consent Informed consent was obtained from all individual participants included in the study.

References

1. Soffietti R, Baumert BG, Bello L, von Deimling A, Duffau H, Frenay M, et al. Guidelines on management of low-grade gliomas: report of an EFNS-EANO task force. Eur J Neurol. 2010;17:1124–33. https://doi.org/10.1111/j.1468-1331.2010.03151.x.
2. Weller M, van den Bent M, Hopkins K, Tonn JC, Stupp R, Falini A, et al. EANO guideline for the diagnosis and treatment of anaplastic gliomas and glioblastoma. Lancet Oncol. 2014;15:e395–403. https://doi.org/10.1016/S1470-2045(14)70011-7.
3. Louis DN, Ohgaki H, Wiestler OD, Cavenee WK, Burger PC, Jouvet A, et al. The 2007 WHO classification of tumours of the central nervous system. Acta Neuropathol. 2007;114:97–109. https://doi.org/10.1007/s00401-007-0243-4.
4. Louis DN, Perry A, Reifenberger G, von Deimling A, Figarella-Branger D, Cavenee WK, et al. The 2016 World Health Organization classification of tumors of the central nervous system: a summary. Acta Neuropathol. 2016;131:803–20. https://doi.org/10.1007/s00401-016-1545-1.
5. Eckel-Passow JE, Lachance DH, Molinaro AM, Walsh KM, Decker PA, Sicotte H, et al. Glioma groups based on 1p/19q, IDH, and TERT promoter mutations in tumors. N Engl J Med. 2015;372:2499–508. https://doi.org/10.1056/NEJMoa1407279.
6. Albert NL, Weller M, Suchorska B, Galldiks N, Soffietti R, Kim MM, et al. Response assessment in neuro-oncology working group and European Association for Neuro-Oncology recommendations for the clinical use of PET imaging in gliomas. Neuro-Oncology. 2016;18:1199–208. https://doi.org/10.1093/neuonc/now058.
7. Pauleit D, Floeth F, Hamacher K, Riemenschneider MJ, Reifenberger G, Muller HW, et al. O-(2-[18F]fluoroethyl)-L-

tyrosine PET combined with MRI improves the diagnostic assessment of cerebral gliomas. Brain. 2005;128:678–87.
8. Jansen NL, Suchorska B, Wenter V, Eigenbrod S, Schmid-Tannwald C, Zwergal A, et al. Dynamic 18F-FET PET in newly diagnosed astrocytic low-grade glioma identifies high-risk patients. J Nucl Med. 2014;55:198–203. https://doi.org/10.2967/jnumed.113.122333.
9. Jansen NL, Suchorska B, Wenter V, Schmid-Tannwald C, Todica A, Eigenbrod S, et al. Prognostic significance of dynamic 18F-FET PET in newly diagnosed astrocytic high-grade glioma. J Nucl Med. 2015;56:9–15. https://doi.org/10.2967/jnumed.114.144675.
10. Lopci E, Riva M, Olivari L, Raneri F, Soffietti R, Piccardo A, et al. Prognostic value of molecular and imaging biomarkers in patients with supratentorial glioma. Eur. J. Nucl. Med. Mol. Imaging. 2017;44:1155–64. https://doi.org/10.1007/s00259-017-3618-3.
11. Verger A, Stoffels G, Bauer EK, Lohmann P, Blau T, Fink GR, et al. Static and dynamic (18)F-FET PET for the characterization of gliomas defined by IDH and 1p/19q status. Eur. J. Nucl. Med. Mol. Imaging. 2018;45:443–51. https://doi.org/10.1007/s00259-017-3846-6.
12. Jansen NL, Graute V, Armbruster L, Suchorska B, Lutz J, Eigenbrod S, et al. MRI-suspected low-grade glioma: is there a need to perform dynamic FET PET? Eur. J. Nucl. Med. Mol. Imaging. 2012;39:1021–9. https://doi.org/10.1007/s00259-012-2109-9.
13. Unterrainer M, Vettermann F, Brendel M, Holzgreve A, Lifschitz M, Zahringer M, et al. Towards standardization of 18F-FET PET imaging: do we need a consistent method of background activity assessment? EJNMMI Res. 2017;7:48. https://doi.org/10.1186/s13550-017-0295-y.
14. Unterrainer M, Schweisthal F, Suchorska B, Wenter V, Schmid-Tannwald C, Fendler WP, et al. Serial 18F-FET PET imaging of primarily 18F-FET-negative glioma: does it make sense? J Nucl Med. 2016;57:1177–82. https://doi.org/10.2967/jnumed.115.171033.
15. Floeth FW, Pauleit D, Sabel M, Stoffels G, Reifenberger G, Riemenschneider MJ, et al. Prognostic value of O-(2-18F-fluoroethyl)-L-tyrosine PET and MRI in low-grade glioma. J Nucl Med. 2007;48:519–27.
16. Suchorska B, Giese A, Biczok A, Unterrainer M, Weller M, Drexler M, et al. Identification of time-to-peak on dynamic 18F-FET-PET as a prognostic marker specifically in IDH1/2 mutant diffuse astrocytoma. Neuro-Oncology. 2018;20:279–88. https://doi.org/10.1093/neuonc/nox153.
17. Olar A, Wani KM, Alfaro-Munoz KD, Heathcock LE, van Thuijl HF, Gilbert MR, et al. IDH mutation status and role of WHO grade and mitotic index in overall survival in grade II-III diffuse gliomas. Acta Neuropathol. 2015;129:585–96. https://doi.org/10.1007/s00401-015-1398-z.
18. Hasselblatt M, Jaber M, Reuss D, Grauer O, Bibo A, Terwey S, et al. Diffuse astrocytoma, IDH-wildtype: a dissolving diagnosis. J Neuropathol Exp Neurol. 2018. https://doi.org/10.1093/jnen/nly012.
19. de la Fuente MI, Young RJ, Rubel J, Rosenblum M, Tisnado J, Briggs S, et al. Integration of 2-hydroxyglutarate-proton magnetic resonance spectroscopy into clinical practice for disease monitoring in isocitrate dehydrogenase-mutant glioma. Neuro-Oncology. 2016;18:283–90. https://doi.org/10.1093/neuonc/nov307.
20. Dang L, White DW, Gross S, Bennett BD, Bittinger MA, Driggers EM, et al. Cancer-associated IDH1 mutations produce 2-hydroxyglutarate. Nature. 2010;465:966. https://doi.org/10.1038/nature09132.
21. Lohmann P, Lerche C, Bauer EK, Steger J, Stoffels G, Blau T, et al. Predicting IDH genotype in gliomas using FET PET radiomics. Sci. Rep. 2018;8:13328. https://doi.org/10.1038/s41598-018-31806-7.
22. Paech D, Windschuh J, Oberhollenzer J, Dreher C, Sahm F, Meissner JE, et al. Assessing the predictability of IDH mutation and MGMT methylation status in glioma patients using relaxation-compensated multi-pool CEST MRI at 7.0 Tesla. Neuro-Oncology. 2018. https://doi.org/10.1093/neuonc/noy073.